Induction of Ocular Complement Activation by Inflammatory Stimuli and Intraocular Inhibition of Complement Factor D in Animal Models

Maura A. Crowley, Omar Delgado, Adrian Will-Orrego, Natasha M. Buchanan, Karen Anderson, Bruce D. Jaffee, Thaddeus P. Dryja, and Sha-Mei Liao

Novartis Institutes for Biomedical Research, Cambridge, Massachusetts, United States

PURPOSE. Genome-wide association studies suggest a role for the complement system in age-related macular degeneration (AMD). We characterized ocular complement activation and evaluated a complement factor D (FD) neutralizing antibody.

METHODS. Mice were treated with toll-like receptor (TLR) ligands, intravitreal injection (IVT), or corneal debridement. Levels of complement proteins and mRNA were measured. A FD neutralizing antibody was administered IVT into eyes of rabbits that were challenged with LPS (lipopolysaccharide) administered intravenously.

RESULTS. Levels of C3 and factor B (FB) mRNA and protein in the eye were increased following intraperitoneal injection of TLR4 ligand LPS. Increased levels of C3 and FB breakdown products were observed in both eye tissues and plasma. Complement activation products were markedly reduced in $C3^{-/-}$ and $Cfb^{-/-}$ mice challenged with LPS. Ocular complement levels were also elevated in mice treated systemically with TLR2 and -3 ligands, injured by IVT injection or corneal debridement, or even in normal aging. IVT administration of a complement FD neutralizing antibody in rabbits inhibited LPS-induced complement activation in the posterior segment of the eye, but not in the anterior segment of the eye or in plasma.

CONCLUSIONS. Systemic TLR stimulation and eye tissue injury induced time-dependent alternative complement pathway activation in the eye. Ocular complement levels were also gradually elevated during aging. An anti-FD antibody IVT potently inhibited LPS-induced complement activation in the posterior segment of the eye. This study provides insights into the dynamic profile of ocular complement activation, which is valuable for complement research in eye diseases and for developing complement therapeutics for AMD.

Keywords: alternative complement pathway, animal model, complement factor D, toll-like receptor

Age-related macular degeneration (AMD) is the leading cause of central vision loss in the aging population. Increasing evidence implicates the involvement of the immune system, specifically abnormalities in the alternative complement pathway (AP), in the pathogenesis of AMD.[1–7] Genetic linkage and genome-wide association studies have identified AMD susceptibility alleles in multiple complement genes (*CFH, CFI, C2/CFB, C3, C9, CFHR1/3*).[8–20] Complement proteins are frequently detected in drusen, the deposits in the macular area that are a common early sign of AMD.[11,21–23] Moderate elevation of complement components and activation products has been reported in plasma and eye samples from AMD patients.[24–31] Multiple animal models of AMD have been utilized, such as laser-induced choroidal neovascularization, light damage–induced retinal degeneration, and cigarette smoke exposure, to assess the role of complement in the eye.[32–38] Several complement inhibitors are currently being tested in the clinic for the treatment of AMD.[39–42] However, the precise mechanism of how complement activation influences AMD disease pathology and progression and even the basic understanding of complement function in the eye are still under investigation.

The AP is a part of the host defense system of innate immunity. It opsonizes and destroys invading pathogens and also responds to endogenous danger signals such as injured or apoptotic cells. Because increased complement activation is associated with AMD pathology,[24–31] identification of factors that activate complement in the eye could have implications for the pathogenic mechanisms of AMD. We characterized the changes in complement levels from eye tissues under various AMD-like pathophysiological conditions in mice. We also evaluated the ability of an intravitreally injected anti-FD antibody to block ocular complement activation in rabbits.

MATERIALS AND METHODS

Animals and Induction of Acute Ocular Inflammation

All animal experiments adhered to the ARVO Statement for the Use of Animals in Ophthalmic and Vision Research and were approved by the Novartis Institutes for Biomedical Research Animal Care and Use Committee. Female C57BL/6 mice were

purchased from Taconic Biosciences (Rensselaer, NY, USA), Charles River Laboratories (Wilmington, MA, USA), and Jackson Laboratory (Bar Harbor, ME, USA). C57BL/6N mice from either Taconic Biosciences or Charles River Laboratories were used in all the mouse studies, except for one aging study with C57BL/6J mice from Jackson Laboratory. C57BL/6N mice from both Taconic Biosciences and Charles River Laboratories are B6N. The rd8 mutation in the *Crb1* gene is present in C57BL/6N mice from both vendors as reported.[43] Animals were housed in a pathogen-free facility on a 12-hour light and dark cycle and were fed standard laboratory chow and sterile water ad libitum. $C3^{-/-}$ (Jackson Laboratory) and $Cfb^{-/-}$ (University of Texas-Houston, Houston, TX, USA) mice and their wild-type (WT) littermates in C57BL/6N background strain were generated by heterozygous breeding.[44,45] Acute ocular inflammation in mice was induced by intraperitoneal (IP) injection of either *Salmonella typhimurium* lipopolysaccharide (LPS) (Sigma-Aldrich Corp., St. Louis, MO, USA), Pam3CSK4 (InvivoGen, San Diego, CA, USA), or poly I:C (polyinosinic-polycytidylic acid, InvivoGen) at the indicated doses formulated in sterile phosphate-buffered saline (PBS). Control animals received an IP injection of sterile PBS. On average, six to eight mice were used per time point in each treatment group. In IVT injection studies in mice, 1 μL sterile PBS was injected per mouse eye. Corneal epithelial debridement was performed as described previously.[46] Male Dutch Belted rabbits at 8 weeks of age were purchased from Covance (Princeton, NJ, USA). Acute ocular inflammation in rabbits was induced by an intravenous injection of 20 μg/kg LPS. Twenty-four hours prior to LPS challenge, either anti-FD antibody (R&D Systems, Minneapolis, MN, USA) or a control goat IgG antibody (R&D Systems) was intravitreally administered bilaterally at 200 μg in 50 μL per eye. On average, five to seven rabbits were used per treatment group.

Tissue Collection and Preparation of Eye RNA and Protein Lysates

For mice, at indicated times post stimuli injection, plasma was collected. Eyes with lens removed were collected and frozen quickly on dry ice. While quickly collecting eye tissues, care was taken to avoid as much ocular muscle as possible. For rabbits, plasma was collected via ear vein 18 hours after LPS injection. Eye tissues were collected step by step on ice-cold petri dishes. First, aqueous humor was collected from enucleated intact eyes by careful drawing into a 3-mL syringe with a 25-gauge needle. Then the cornea was dissected away and iris/ciliary body (CB) were collected. The lens was removed next and vitreous humor was collected using a 1-mL pipette tip. After all the vitreous was carefully removed, the eye cup consisting of retina and retinal pigment epithelium (RPE) and choroid was collected with a number 21 scalpel. Each tissue was immediately placed on dry ice right after collection. All disposable tools were used once; other tools were cleaned between each tissue dissection to avoid cross-contamination. Total RNA was isolated from homogenized eye tissues using RNeasy micro columns (Qiagen, Venlo, Netherlands). Cell lysis buffer from Cell Signaling Technology (Danvers, MA, USA) was used to prepare eye protein lysates. Mouse eye tissues were dissociated in 200 μL lysis buffer. Rabbit iris/CB and retina/RPE/choroid were dissociated in 250 and 500 μL, respectively. Eye tissues were lysed using a TissueLyser II (Qiagen). The Bradford protein assay (ThermoFisher, Waltham, MA, USA) was used to determine protein concentrations of respective samples.

TaqMan

One microgram DNase I–treated total RNA from each eye sample was reverse-transcribed using the High Capacity cDNA Reverse Transcription kits (Applied Biosystems, Waltham, MA, USA). Reverse-transcribed cDNA was used for TaqMan quantitative real-time PCR reactions. Expression of the gene of interest was determined on the ABI Prism 7900HT (Applied Biosystems) with TaqMan mouse GAPDH endogenous control reagents. Primers used for real-time PCR purchased from Invitrogen (Waltham, MA, USA) were mouse *C3* (Mm01232779_m) and mouse *Cfb* (Mm00433909_m1). The ΔC_t value was calculated by subtracting the GAPDH C_t from the gene of interest C_t. The relative expression of the gene of interest $= 2^{-\Delta Ct}$ divided by the average of PBS control $2^{-\Delta Ct}$.

Protein Gel and Western Blot

Equal amounts of eye protein extract (40–60 μg protein) or 0.5 μL plasma from each sample was resolved on SDS gels (Novex NuPAGE 4-12% Bis-Tris; Invitrogen), and then transferred onto nitrocellulose membranes (iBlot Gel Transfer Stacks Nitrocellulose, Invitrogen). After incubation with Odyssey blocking buffer (LI-COR, Lincoln, NE, USA), the nitrocellulose membranes were probed with primary antibodies: either anti-mouse C3d (R&D Systems) or anti-factor B (FB) antibody (Quidel, San Diego, CA, USA). Secondary antibody was infrared fluorescently conjugated anti-goat antibody (IRDye800CW donkey anti-Goat IgG; Rockland, Limerick, PA, USA). Infrared fluorescent signals, which are directly proportional to the amount of the antigen on the Western blots, were detected with the Odyssey imager (LI-COR) and quantified using Odyssey software.

C3a and C5a MSD

Standard MSD plates (Meso Scale Discovery, Rockville, MD, USA) were coated with rat anti-mouse C3a or C5a (BD Pharmingen 558250 or 558027; East Rutherford, NJ, USA). Diluted mouse plasma and eye lysates that had been normalized to 5 mg protein/mL lysis buffer were added to MSD plates. Mouse C3a and C5a proteins (BD Pharmingen 558618; R&D Systems 2150-C5) were used to generate standard curves. Secondary biotinylated anti-mouse C3a or C5a antibody (BD Pharmingen 558251; R&D Systems BAF2150) and detection antibody (streptavidin-sulfotag, Meso Scale Discovery) were used and plates were read on a MSD plate reader.

Complement Alternative Pathway Functional Assay

Black MaxiSorp (Thermo Scientific, Waltham, MA, USA) plates were coated with Zymosan A (Sigma-Aldrich Corp.) diluted to 1 mg/mL in carbonate buffer pH 9.5 (Thermo Scientific) and washed three times with TBS-Tween 20 (TBS-T) buffer. A 7-point serial dilution of anti-human FD goat polyclonal antibody (AF1824, R&D Systems) starting at a concentration of 130 nM (final concentration in reaction) was prepared in saline. Normal human serum (Quidel) or normal rabbit serum (BioreclamationIVT, New Cassel, NY, USA) was diluted to 6% in ice-cold GVB-MG buffer (Boston Bioproducts, Ashland, MA, USA) supplemented to 2 mM MgCl₂ final concentration for alternative pathway conditions. Diluted serum was first added to a polypropylene plate, and then diluted antibody was added. The plate was incubated for 15 minutes at room temperature, followed by transfer of 25 μL of the mixture to the coated reaction plate. The reaction plate was sealed with a plastic

adhesive film and incubated at 37°C for 30 minutes. The reaction was terminated by washing the plate three times with TBS-T. Membrane-attack complex (MAC) was detected with an alkaline phosphatase–conjugated mouse anti-human C9 neo-epitope monoclonal antibody (clone AE11; Diatec, Oslo, Norway) at 0.25 µg/mL. The plate was incubated for 1 hour at room temperature. After washing three times with TBS-T, substrate 4-MUP (Fisher, Waltham, MA, USA) at 0.18 mg/mL in 0.1 M Tris-HCl pH 9.0 containing 2 mM $MgCl_2$ was added and the plate was incubated for 30 minutes at room temperature protected from light. Plates were read at 355-nm excitation/460-nm emission on a Fluoroskan plate reader (Thermo Scientific). Percentage inhibition of MAC deposition was calculated relative to the positive control (serum with assay buffer) after subtracting the background signal (serum with 25 mM EDTA added). These data were used to generate the IC_{50} value using nonlinear regression with GraphPad Prism software (GraphPad Prism, LaJolla, CA, USA).

Statistical Data Analysis

Data are presented as mean ± SEM. Mean differences were compared and statistical differences were determined by 2-tailed unpaired *t*-test. Differences were considered statistically significant when $P < 0.05$.

For FD antibody studies in rabbits, data were analyzed by subtracting the baseline values of the Ba levels (control IgG and PBS-treated group) from all values for each LPS-treated group. Using the baseline-subtracted values, the percent inhibition was calculated as % inhibition = (1 − [value of Ba with anti-FD Ab and LPS/average value of Ba in control IgG and LPS group]) × 100.

Results

Systemic Administration of LPS Induces Transient Complement Synthesis and Activation in Mouse Eyes

Toll-like receptor (TLR) activation has been proposed to contribute to AMD pathology.[5,47] LPS, the major cell wall component of Gram negative bacteria, is a potent activator of TLR4. Endotoxin/LPS-induced uveitis (EIU) has been used as an acute model to evaluate anti-inflammatory reagents, such as anti-TNFα.[48,49] To assess the effect of acute systemic TLR4 activation on complement activation in the eye, LPS was administered via IP injection in C57BL/6N mice. Plasma and eye tissues were collected at various time points from 3 hours to 14 days after a single LPS treatment. Levels of ocular *C3* and *Cfb* mRNA measured by TaqMan peaked 16 hours post LPS, and increased 20- to 50-fold, compared to the level of PBS-treated controls (Figs. 1A, 1B). Systemic LPS therefore induces local complement synthesis in eye tissues.

Western blots were used to evaluate the effect of LPS on AP proteins in mouse plasma and eye tissues. Representative Western blot images are presented in Figures 1C and 1D. Full-length C3 (~120 kDa) and FB (~90 kDa) protein levels were increased in eye tissues, peaking at 24 to 48 hours post LPS challenge at levels 2- to 3-fold higher than in PBS-treated control animals (Figs. 1A, 1B). The 10- to 20-fold difference between induced mRNA and protein levels is likely due to LPS-induced complement activation that results in breakdown of full-length C3 and FB proteins. Similar induction of full-length C3 and FB proteins was observed in plasma (data not shown).

The alternative pathway of the complement system is activated by a cascade of proteolytic steps. The FD protease cleaves FB into Bb and Ba. Bb serves as the catalytic subunit of C3 convertase (C3bBb) and splits C3 alpha into C3a and C3b. A majority of C3b is rapidly cleaved into iC3b, which is further degraded into C3d. A small portion of C3b binds to C3bBb to form the C5 convertase, which breaks down C5 into C5a and C5b. We evaluated these breakdown products to determine optimal readouts for complement activation in vivo. In naïve or PBS-treated control mice, Ba, C3d, and iC3b were barely detectable in eye tissues while a low level of each was present in plasma due to the continuous tick-over process of C3 cleavage by $C3(H_2O)FB$.[50-52] Systemic injection of LPS induced a time-dependent increase of Ba, C3d, and iC3b levels in both plasma and eye tissues (Figs. 1E, 1F). Since the C3b level is usually very low, the sum of iC3b and C3d levels was used to represent total C3 breakdown products. Levels of C3 and FB breakdown products increased gradually, starting at 3 hours post LPS challenge, reaching the highest levels at 24 to 48 hours, and thereafter gradually declining. Maximum induction of Ba or C3d+iC3b by LPS was approximately 4- to 6-fold when compared to PBS-treated controls. In plasma, the level of iC3b was approximately 5-fold lower than the C3d level (Fig. 1G). However, in eye tissues, C3d and iC3b levels were comparable, indicating that iC3b may be more stable in the eye than in circulation. C3a and C5a levels, measured by MSD assays, also increased in plasma in a time-dependent manner, but were largely undetectable in eye tissue (Figs. 1H, 1I). C3a and C5a are known to be short-lived in vivo.[53] Therefore, C3 and FB breakdown products Ba, C3d, and iC3b were suitable to monitor both ocular and systemic complement activation from tissue and plasma samples.

LPS induces *C3* mRNA synthesis (Fig. 1A) and C3 protein breakdown (Fig. 1E). C3 is the convergence point of all three complement pathways (classical, alternative, and lectin). Increased *Cfb* mRNA levels (Fig. 1B) and increased complement breakdown product Ba (Fig. 1E) indicate that LPS-induced complement activation involves the alternative pathway and the amplification loop in the common pathway downstream of C3 activation. The role of the complement system in LPS-induced complement activation was further investigated by the use of C3-deficient and FB-deficient mice. Both strains are in C57BL/6N background. Ba levels are undetectable in $C3^{-/-}$ mouse eyes and plasma even following LPS challenge (Figs. 2A, 2B), indicating that C3 is essential for initiation of FB breakdown. C3b or $C3H_2O$ in C3FB complex was considered to be essential for FD to recognize FB and to cleave FB in in vitro studies.[54,55] Using FB breakdown product Ba to monitor FB activation in C3-deficient mice, our data provided in vivo evidence that C3 is required for FB activation. $Cfb^{-/-}$ mice exhibited a significant ($P < 0.01$) but not complete reduction in C3 breakdown products C3d and iC3b in eyes and plasma comparing between LPS-challenged $Cfb^{-/-}$ and WT animals (Figs. 2C, 2D), indicating that the alternative pathway contributes to LPS-induced ocular complement activation.

TLR2 and TLR3 Ligands Also Induce Complement Activation in the Eye

LPS, the major ligand for TLR4, not only induces complement activation but also induces complement synthesis through the TLR4 signaling pathway. To address whether other TLR signaling pathways could also activate complement in the eye, Pam3CSK4 (a synthetic triacylated lipopeptide) and poly I:C (polyinosinic-polycytidylic acid) were evaluated. Pam3CSK4 binds TLR2 and poly I:C signals through TLR3 and other intracellular RNA binding factors. Time-course studies in 7-week-old C57BL/6N mice challenged with IP injection of either Pam3CSK4 or poly I:C exhibited similar patterns of complement synthesis and activation, peaking in both eye and plasma at 8 to 24 hours (Figs. 3A, 3B), although at lower levels of induction compared to LPS challenge. *Cfb*
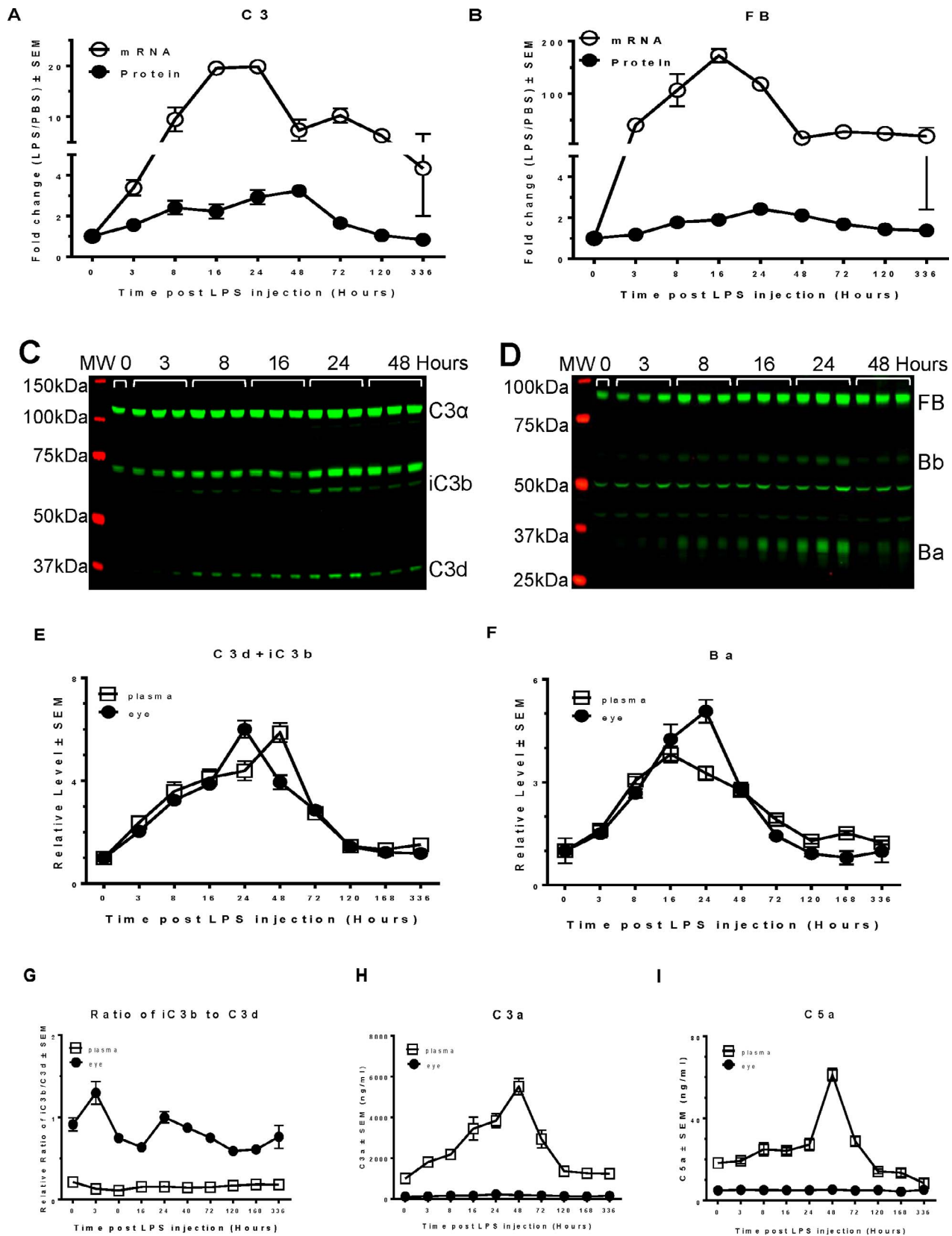
FIGURE 1. Time-dependent induction of complement mRNA and protein following LPS IP injection (2.5 mg/kg) in 7-week-old C57BL/6N mice. The dose of LPS was chosen based on both literature[83] and dose–response studies for the optimal inflammatory responses without producing septic shock (data not shown). (**A**, **B**) *C3* and *Cfb* mRNA levels in eye tissues were graphed relative to PBS-treated controls. Both *C3* and *Cfb* mRNA levels peaked at 16 to 24 hours post LPS IP ($P < 0.001$). Full-length protein levels of complement components C3 and FB were graphed relative to the average value of PBS-treated controls. C3 and FB proteins peaked in eye tissues 48 hours ($P < 0.01$) and 24 hours ($P < 0.001$), respectively, post LPS. (**C**, **D**) Western blot analysis of eye lysates probed for C3 and FB proteins, both full-length proteins and breakdown products. The C3d antibody recognizes any mouse C3d containing

proteins from the full-length C3 alpha chain (~120 kDa) to C3 cleavage fragments C3b, iC3b (~68 kDa), and C3d (~41 kDa). The polyclonal FB antibody recognizes mouse and rabbit full-length FB protein (~90 kDa) and FB cleavage fragments Bb (~60 kDa) and Ba (~30 kDa). (**E, F**) C3 breakdown products C3d+iC3b peaked 24 hours ($P < 0.001$) in eye tissues and 48 hours ($P < 0.001$) in plasma post LPS challenge. FB breakdown product Ba peaked 24 hours ($P < 0.001$) in eye tissues and 16 hours ($P < 0.001$) in plasma post LPS. C3d+iC3b and Ba are graphed relative to PBS-treated controls. (**G**) Ratio of iC3b to C3d is higher in eye than in plasma. Fluorescence intensity of iC3b band was divided by that of C3d band in each sample. (**H, I**) Both complement C3 and C5 breakdown products C3a and C5a peaked 48 hours ($P < 0.001$) post LPS in plasma. The amounts of C3a and C5a were expressed as the levels at 1 mg total protein of the eye lysate/mL lysis buffer. Protein levels of full-length C3 and FB as well as breakdown products C3d, iC3b, and Ba were measured in Western blots. Mouse C3a and C5a were measured by MSD immunoassays. This study is a representative of three independent studies.
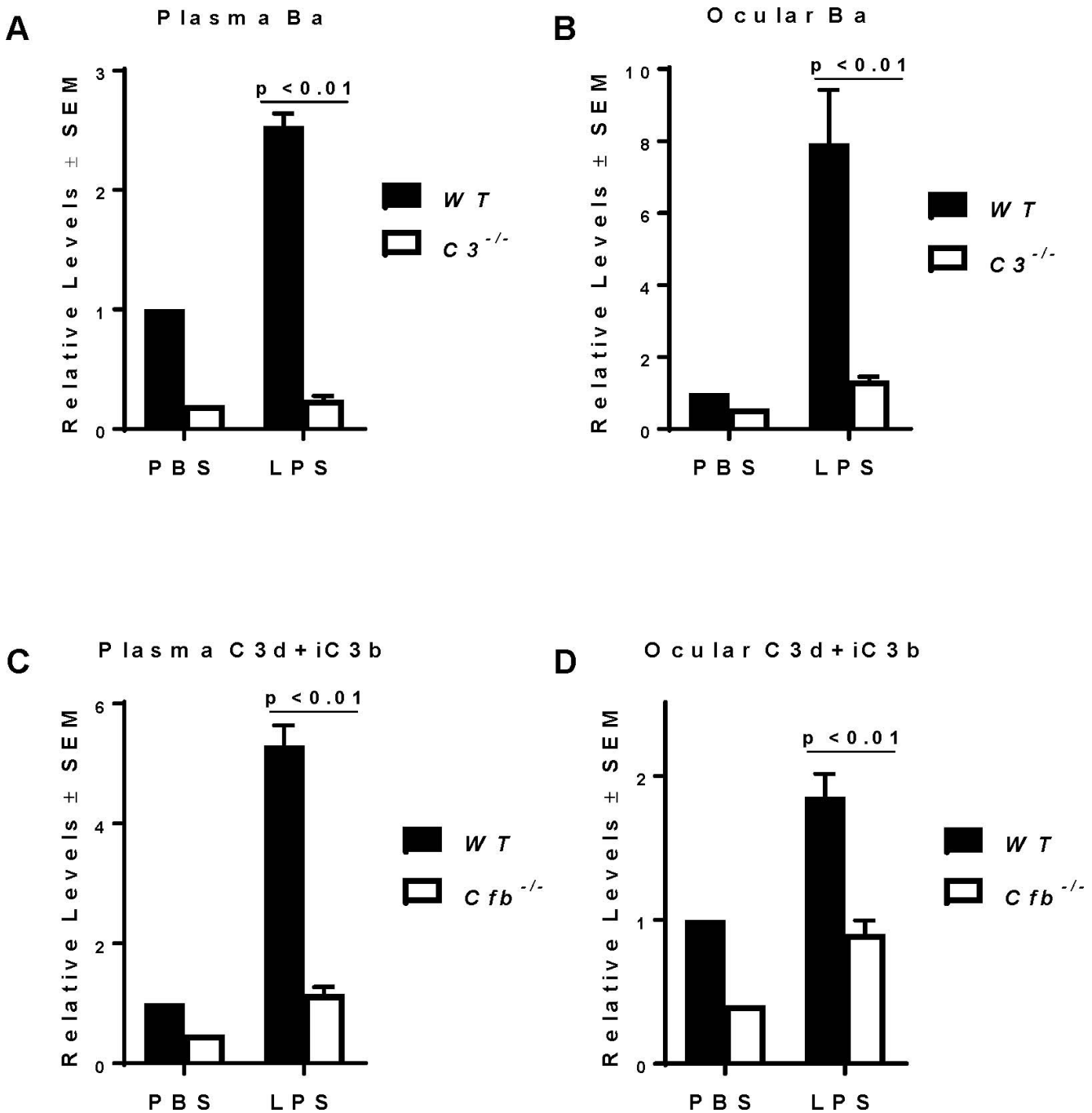
FIGURE 2. LPS-induced complement activation is dependent on the presence of C3 and FB. In order to run all samples on one gel (total 16 wells) for direct comparison between WT and complement-deficient mice in Western blots, seven PBS-treated samples of WT mice were pooled and loaded in 1 well. LPS-treated WT samples were run individually in seven wells. $C3^{-/-}$ or $Cfb^{-/-}$ samples were run in the same manner. The same amounts of protein lysate were loaded in each well. C3 and FB breakdown products C3d, iC3d, and Ba were measured in Western blots and were graphed relative to the average value of PBS-treated WT controls. (**A, B**) Comparing to LPS-treated WT controls, $C3^{-/-}$ mice exhibited a significant reduction ($P < 0.01$) in plasma and ocular Ba levels 24 hours after LPS IP injection (2.5 mg/kg). This is a representative of four independent studies. (**C, D**) Comparing to LPS-treated WT controls, $Cfb^{-/-}$ mice exhibited a significant reduction ($P < 0.01$) in plasma and ocular C3d and iC3b levels 24 hours after LPS IP injection. This is a representative of three independent studies.
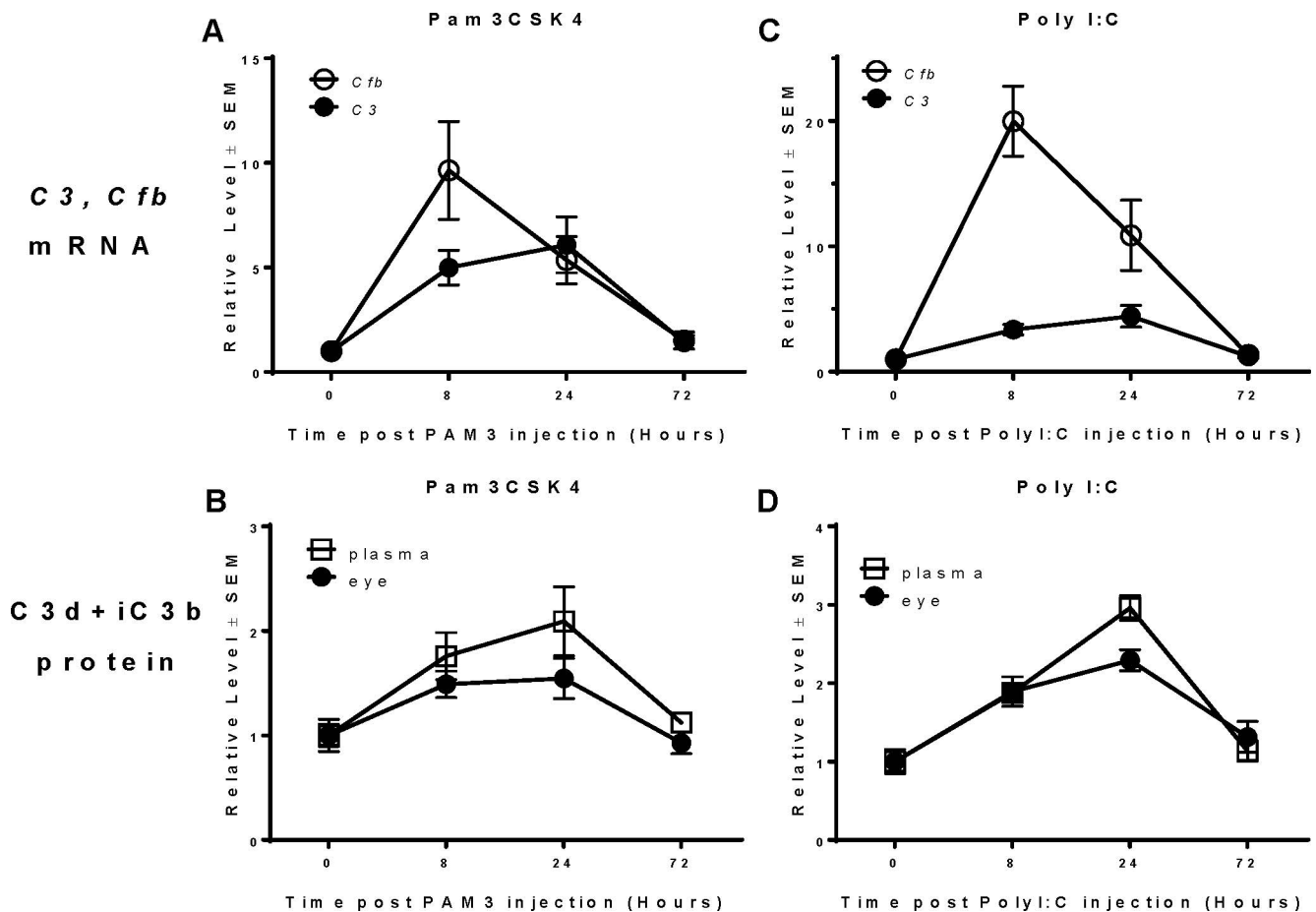
FIGURE 3. TLR2/3 stimulation induces complement synthesis and activation in mouse eyes. TLR2 ligand Pam3CSK4 (1.25 mg/kg) and TLR3 ligand poly I:C (2.5 mg/kg) were administered intraperitoneally to 7-week-old C57BL/6N mice. The doses of Pam3CSK4 and poly I:C were chosen based on both literature and dose–response studies for the optimal inflammatory responses (data not shown).[84–86] Eyes and plasma were collected 0, 8, 24, and 72 hours post injection. *C3* and *Cfb* mRNAs and C3 breakdown products were graphed relative to the average value of PBS-treated controls. **(A)** Pam3CSK4 induced *Cfb* mRNA production in eye tissues, peaking early at 8 hours ($P < 0.05$), while *C3* mRNA peaked at 24 hours ($P < 0.05$) post challenge. **(B)** Poly I:C induced *Cfb* mRNA in eye tissues, peaking early at 8 hours ($P < 0.001$), while *C3* mRNA peaked at 24 hours ($P < 0.01$) post challenge. This study is a representative of four independent studies. **(C)** Similar to TLR4 ligand LPS, Pam3CSK4 induced complement protein activation (levels of iC3b+C3d), peaking at 24 hours in eye tissues and ($P < 0.05$) in plasma. **(D)** Poly I:C induced complement protein activation (levels of iC3b+C3d), peaking at 24 hours ($P < 0.001$) in eye tissues and ($P < 0.001$) in plasma. This study is a representative of four independent studies.

mRNA was generated in the eye at earlier time points and at a higher level compared to *C3* mRNA (Figs. 3C, 3D, 1B), suggesting that TLR signaling may preferentially activate the AP in the eye. Taken together, systemic and ocular complement activation can occur via systemic induction of TLR2, -3, or -4 signaling pathways.

Eye Tissue Damage Induces Rapid and Transient Local Complement Activation

Complement is known to be activated by trauma and in ischemia–reperfusion injury, presumably in response to endogenous danger signals.[56] Intravitreal injection (IVT) is a common procedure to deliver anti-VEGF biologics for neovascular AMD. It involves a needle breaking through normal intact eye surface and retina to reach the vitreous cavity. To address whether ocular complement was affected in response to the danger signals generated in the eye by IVT-associated local tissue damage, ocular complement levels were measured at various time points after a single IVT injection of mouse eyes. Complement breakdown products C3d and iC3b were increased, peaking 4 hours post injection (Fig. 4A). The onset of complement activation triggered

by IVT was more rapid than activation induced by systemic TLR ligands and did not appear to involve enhanced local complement synthesis since the amount of full-length C3 protein in the eye remained unchanged.

Corneal epithelial debridement is a model of inflammatory corneal neovascularization.[46] This model is initiated by mechanically removing the corneal epithelium of C57BL/6N mice. Eye samples were collected at various time points post corneal epithelial debridement, and complement levels were assessed. Similar to IVT, complement breakdown products C3d and iC3b were quickly elevated 2 hours post debridement and returned to baseline by 4 hours (Fig. 4B).

These results demonstrate that eye tissue damage causes rapid and transient local complement activation. Systemic complement levels were not affected by either challenge (data not shown).

Aging Increases Baseline Complement Levels While Decreasing Response to LPS

Aging is the greatest risk factor for AMD and other age-related diseases. We evaluated complement activation during aging in

A

B
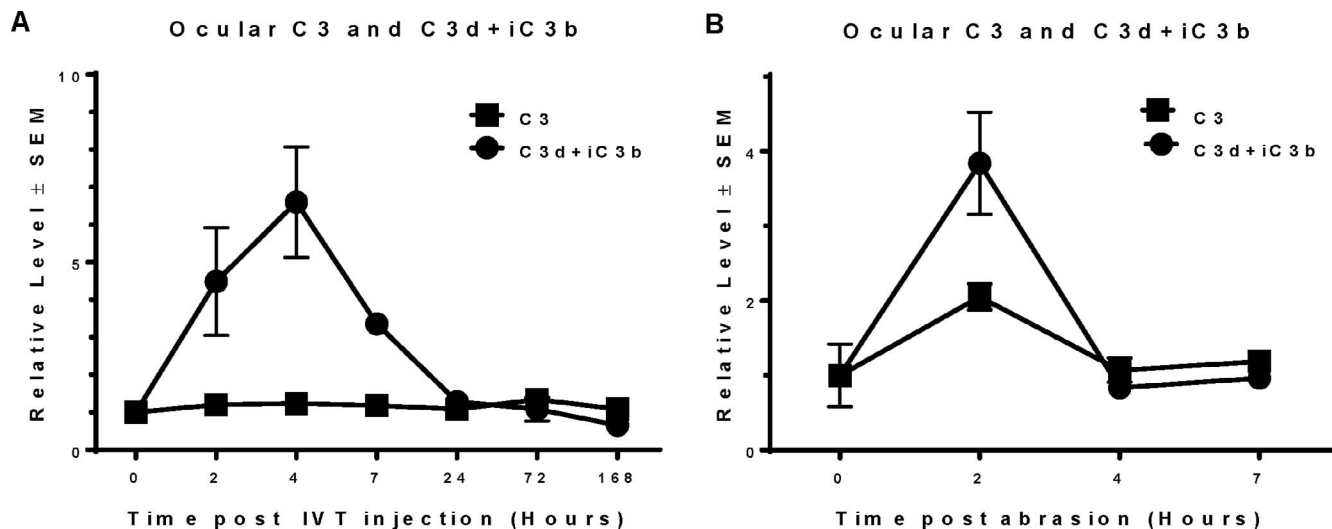
FIGURE 4. IVT injection and corneal debridement induce ocular complement activation in 7-week-old C57BL/6N mice. Eye tissues were collected at indicated time points after treatment. C3 full-length protein and C3 breakdown products were graphed relative to the average value of untreated controls. (**A**) Complement C3 breakdown products increased rapidly after intravitreal injection of 1 μL PBS, peaking 4 hours ($P < 0.01$) post treatment. This study is a representative of two independent studies. (**B**) C3 breakdown products also increased rapidly after corneal debridement, peaking 2 hours ($P < 0.01$) post treatment. This study was performed once.

naïve C57BL/6N mice at 7, 21, and 48 weeks of age. Baseline levels of complement C3 and FB breakdown products gradually increased by 50% to 100% in eye tissues and 50% in plasma from 7 to 48 weeks old, indicating an increase of ocular and systemic complement activation with age (Figs. 5A, 5B). Aged C57BL/6N mice were reported to have increased accumulation of subretinal microglia/macrophages likely due to the presence of the rd8 mutation in the *Crb1* gene.[57] To address if the rd8 mutation plays a role in complement activation, we evaluated complement activation during aging in naïve C57BL/6J mice, which do not carry the rd8 mutation, at 7, 22, and 54 weeks of age. Baseline levels of complement C3 and FB breakdown products gradually increased by 50% in both eye lysates and plasma from 7 to 54 weeks old, confirming an increase of complement activation with age that is independent of the rd8 mutation (Figs. 5C, 5D). Additionally, the ability to mount a response to LPS was reduced in older C57BL/6N mice. Complement breakdown products in eye tissues following LPS challenge were increased 5- to 8-fold in 7-week-old mice, but only 2- to 3-fold in 48-week-old mice (Fig. 5E). There was also a moderate reduction in LPS response in the plasma from 7 to 48 weeks old (Fig. 5F).

Factor D (FD) Neutralizing Antibody Inhibits Local Complement Activation in Rabbits

Human and rabbit FD proteins share 81% amino acid identity. A commercially available anti-human FD antibody from R&D Systems neutralized both human and rabbit FD in human and rabbit serum-based alternative pathway assays with similar potencies (Fig. 6A). However, possibly due to limited sequence homology between mouse and human FD proteins (66% identity), the anti-human FD antibody failed to inhibit AP complement activation in a similar assay with mouse serum (not shown). LPS-induced complement activation was adapted from mouse to rabbit to enable evaluation of the human FD neutralizing antibody via intravitreal delivery. The larger eye of rabbits is more suitable for preclinical testing of intraocular delivery of biologics with longer half-life. Since FB is the substrate for FD, the soluble FB breakdown product Ba was used as a direct readout for FD inhibition. Eighteen hours after

LPS injection, the level of Ba in the posterior segment of the eye (retina/RPE/choroid) was 2- to 3-fold above PBS-treated controls. LPS-induced Ba generation in the posterior segment of the eye was inhibited by intravitreal administration of the anti-human FD antibody at 200 μg per eye 24 hours before LPS challenge. We assume that the concentration of FD in the eye should be lower than in serum (40–80 nM)[58] and rabbit vitreous volume to be around 1.52 cm^3.[59] Intravitreal injection of 200 μg per eye would predict ~0.88 μM anti-FD, which is at least 11- to 22-fold higher than FD levels in the vitreous. LPS-induced alternative pathway activation in vitreous humor as measured by Ba generation was completely blocked (Fig. 6B) 42 hours after IVT of the anti-FD antibody. There was a 60% reduction of Ba levels in the retina/RPE/choroid (Fig. 6C). Since choroid is a highly vascular tissue, some of the Ba fragments detected in retina/RPE/choroid may have come from the blood. As expected, LPS-induced Ba generation in plasma was not affected by IVT anti-FD (Fig. 6D). LPS-induced Ba generation in the anterior segment of the eye (aqueous humor or iris/CB) was also unaltered by FD antibody pretreatment (Figs. 6E, 6F). This result demonstrates for the first time in rabbits that intravitreal administration of a complement inhibitor blocks local complement activation while complement levels in systemic circulation or even the adjacent tissue compartment remain unaffected.

DISCUSSION

Despite the strong genetic association with AMD and increasing evidence that upregulation of complement activation is associated with AMD pathology,[24–31] little is known about how complement is activated in the eye. This is partly due to the lack of tools to monitor complement activity, particularly in eye tissue. Having established quantitative MSD immunoassays and Western blot assays, we were able to profile ocular and systemic alternative pathway complement activation under potential AMD-like pathophysiological conditions in mice. We demonstrated that multiple endogenous and exogenous danger signals that induce the innate immune system are capable of activating complement in the eye. Among them, aging is a well-known risk factor for AMD. TLR
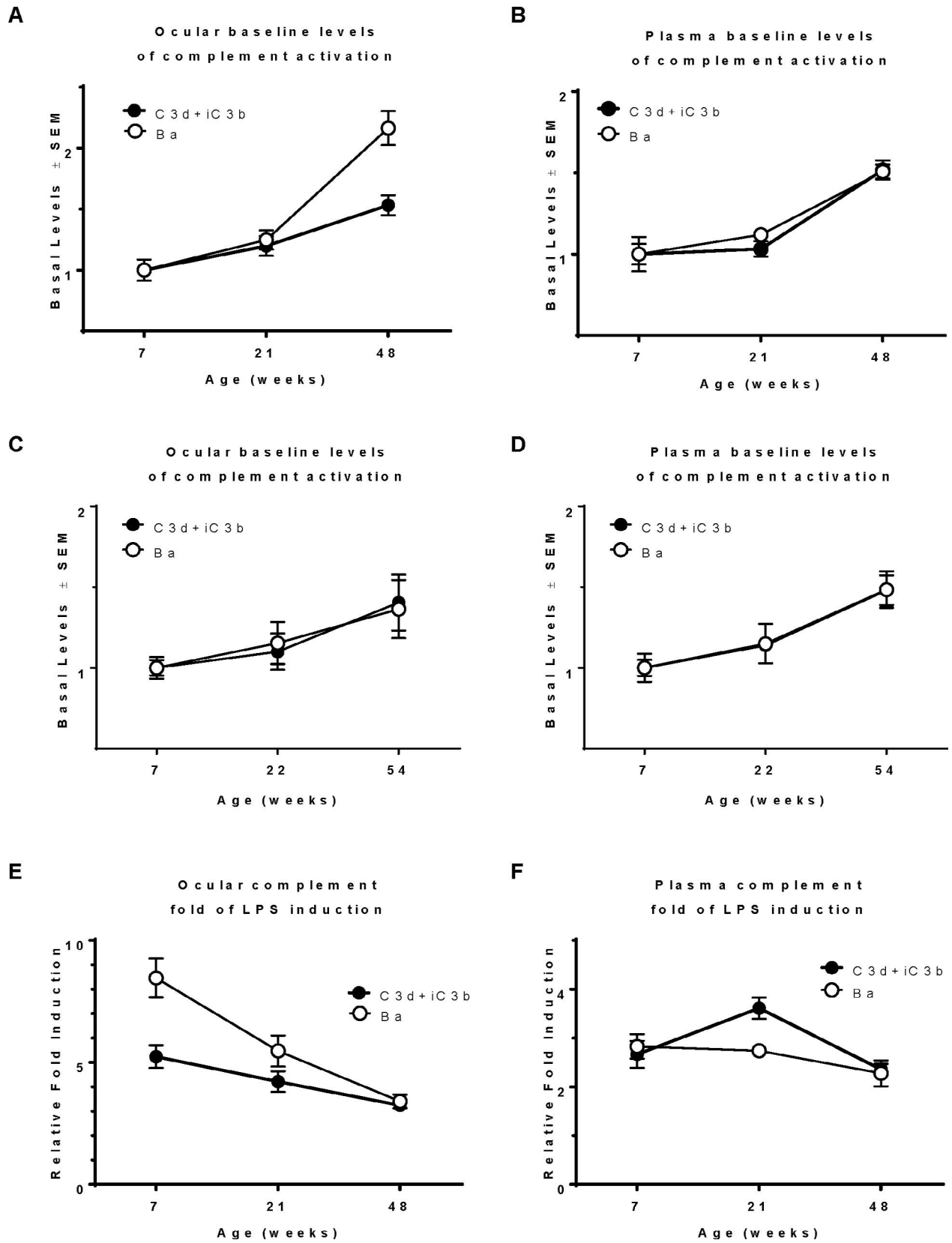
FIGURE 5. Effect of aging on complement activation. Complement breakdown products Ba, C3d, and iC3b were assessed from naïve and LPS IP-injected C57BL/6N female mice at 7, 21, and 48 weeks of age and from naïve C57BL/6J female mice at 7, 22, and 54 weeks of age. LPS treatment was 24 hours. C3 and FB breakdown products were measured by Western blots and were graphed relative to the average value of 7-week-old samples. (**A**) Baseline levels of complement activation products in eye tissues of C57BL/6N mice increased with age from 7 to 48 weeks ($P < 0.001$ for C3d+iC3b and $P < 0.001$ for Ba). (**B**) Baseline levels of complement activation products in plasma of C57BL/6N mice also increased with age from 7 to 48 weeks ($P < 0.01$ for C3d+iC3b and $P < 0.01$ for Ba). (**C**) Baseline levels of complement activation products in eye tissues of C57BL/6J mice

increased with age from 7 to 54 weeks ($P < 0.05$ for C3d+iC3b). (**D**) Baseline levels of complement activation products in plasma of C57BL/6J mice also increased with age from 7 to 54 weeks ($P < 0.001$ for C3d+iC3b and $P < 0.01$ for Ba). The fold induction, which is the ratio of LPS-induced to baseline complement activation products, decreased with age in eye tissues (**E**) and plasma (**F**) in C57BL/6N mice. In eye tissues, induction of complement breakdown products by LPS was reduced by 60% ($P < 0.001$) for Ba and 39% ($P < 0.01$) for C3d+iC3b from 7 to 48 weeks of age. This is a representative of four independent studies with C57BL/6N mice. The baseline aging study with C57BL/6J mice was performed once.

---

activation by pathogen products has also been implicated in AMD pathology.[5,47] Furthermore, the stress response to eye tissue damage by the examples of IVT injection or corneal debridement could easily trigger complement activation. AMD is a complex and multifactorial disease, and complement activation could be a common pathogenic mechanism influenced by multiple AMD risk factors.

Most complement components are produced in the liver and circulate in the bloodstream as one of the main defense mechanisms against pathogens and endogenous danger signals. The role of complement activation in the eye is less well understood. Our results identify at least two types of local ocular complement activation induced by either eye tissue damage or systemic TLR activation. Local acute injury such as an IVT or corneal debridement breaks down the barrier between eye tissue and capillary blood vessels. This may cause a transient influx of complement proteins from blood, which, in combination with the presence of low levels of complement components in the eye, may lead to rapid ocular complement activation. Systemic challenge with TLR ligands may not directly activate ocular complement. Instead, TLR ligands upregulate complement gene expression in the eye, which leads to a slow induction of ocular complement activation, peaking 24 hours post challenge. Although some of the ocular complement activation by systemic TLRs might be due to residual blood from tissue collection, we observed similar levels of LPS-induced complement activation in eye tissue with or without removal of blood by perfusion (not shown). In addition, local complement inhibition would not be able to block complement breakdown products coming from circulation. The IVT FD antibody in this study inhibited complement activation in the eye, but not in the blood. This indicates that the ocular activation products are generated locally. The increased levels of C3 and FB mRNA and protein in the eye after inflammation could be produced by the infiltrating neutrophils and monocytes since leukocytes are good complement producers.[60,61] They could be also synthesized by resident cells such as microglia, astrocytes, and RPE cells.[62–66]
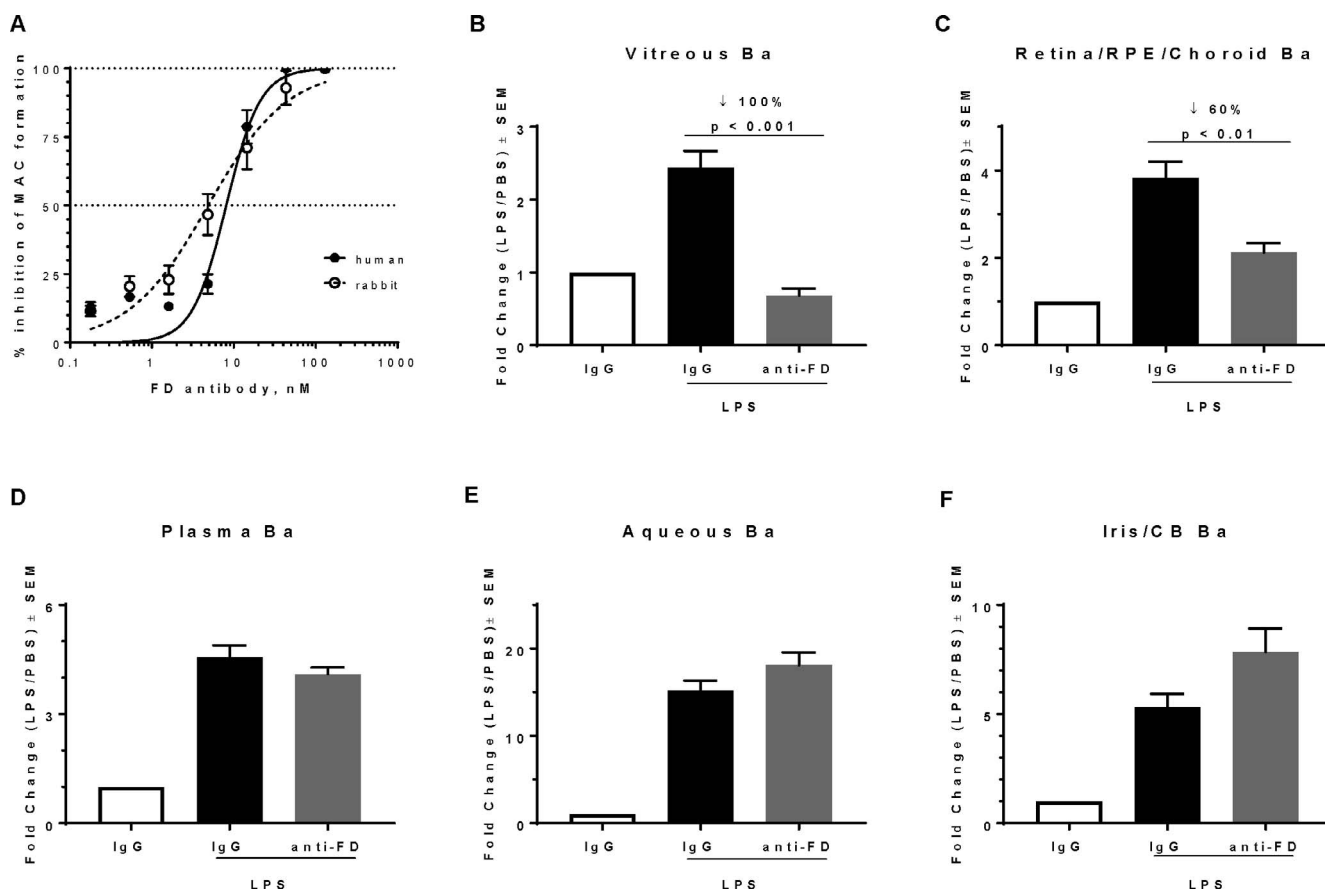
FIGURE 6. Intravitreal administration of an antibody against complement factor D inhibits LPS-induced Ba generation in rabbits in the posterior segment of the eye, but not systemically or in the anterior segment of the eye. (**A**) MAC deposition after Zymosan-induced alternative pathway activation in 6% human serum (*solid line*) or rabbit serum (*dotted line*) was blocked by a FD-neutralizing polyclonal antibody with IC$_{50}$ values of 8.1 and 4.9 nM, respectively. Twenty-four hours before LPS challenge, goat IgG or anti-FD was delivered IVT at 200 μg per eye to both eyes. Eighteen hours after intravenous injection of either PBS or LPS at 20 μg/kg, plasma (**D**) and eye tissue were collected. Eyes were dissected immediately into vitreous humor (**B**), retina/RPE/choroid (**C**), aqueous humor (**E**), and iris/ciliary (CB) (**F**). Complement Ba levels in indicated tissues were measured by Western blot and graphed relative to the IgG/PBS control group. LPS-induced Ba generation was inhibited 100% ($P < 0.01$) in vitreous humor and was reduced by 60% ($P < 0.01$) of PBS control levels in retina/RPE/choroid. The rabbit LPS study is a representative of two independent studies.

The eye is considered an immunoprivileged site where complement is under tight control by intraocular complement regulators.[42,67] However, we found that complement levels in the eye are easily altered in response to various inflammatory perturbations. Frequent exposure to systemic or local inflammatory stimuli, such as TLR ligands derived from pathogen products or damaged tissue components, in combination with 50 to 60 years of aging could lead to a constant low level of complement activation in the eye, ultimately contributing to the development of AMD. This may be particularly relevant for those who are predisposed with high-AMD-risk genetic variants in complement genes.[27]

A notable difference we observed between systemic and ocular complement activation in mice is the higher level of iC3b relative to C3d level in eye tissues. The average ratio of ocular iC3b to C3d is 5-fold higher than in plasma. Plasma iC3b is barely detectable, while the ocular iC3b level is always comparable to the ocular C3d level. Increased deposition of iC3b along the glomerular basement membrane in complement factor H–deficient mice is responsible for the detrimental effect on renal function in the murine model of dense deposit renal disease.[68] The interaction between iC3b and its receptor complement receptor 3 (CR3) is likely to play a similar role in the early synapse loss in Alzheimer mouse models.[69] The presence of iC3b in drusen and on RPE cells has been proposed as one of the pathogenic mechanisms of AMD.[70,71] Deposition of iC3b on the ocular cell surface could be recognized by infiltrating phagocytes or resident microglia that express CR3 or CR4, leading to macrophage activation and phagocytic damage to ocular cells such as RPE and photoreceptors. The presence of macrophages and subretinal microglia cells has been reported in AMD eyes.[72–75]

Currently a number of complement therapies are in clinical trials for AMD.[40,76] Lampalizumab, an anti-complement FD Fab (IVT), is in phase 3 clinical trials for the treatment of geographic atrophy (GA), an advanced form of AMD.[77–80] However, Genentech recently announced that lampalizumab failed in one of the two phase 3 GA trials.[81] Blocking complement FD, the first protease in the AP cascade, will prevent the generation of multiple inflammatory components in the alternative pathway and in the amplification loop. The effect of lampalizumab IVT on systemic complement activation was reported, but not its efficacy against complement activation in the eye.[82] We demonstrated that complement activation in the vitreous was completely blocked 2 days after IVT of an IgG anti-human FD antibody in rabbits. However, in the retina/RPE/choroid fraction, which is considered to be the site of action for complement in the pathogenesis of AMD, only 60% inhibition was observed, possibly due to residual systemic complement products in choroidal and retinal vessels without PBS perfusion. Another possibility would be partial inhibition of local complement likely due to incomplete penetration of the antibody into the ocular tissues from vitreous. Thus the contribution of complement from choroidal and retinal vessels may account for only at most 40% of the total complement observed. Since only a modest increase in complement products is observed in AMD patients,[24–31] it remains to be determined how much complement inhibition in eye and/or blood is required to achieve clinical efficacy in AMD trials. Complement model systems that we have developed, in combination with clinical results from complement trials, will be valuable to further understand the role of complement in AMD pathogenesis to design better complement therapeutics.

Acknowledgments

Disclosure: **M.A. Crowley**, Novartis (E); **O. Delgado**, Novartis (E); **A. Will-Orrego**, Novartis (E); **N.M. Buchanan**, Novartis (E); **K. Anderson**, Novartis (E); **B.D. Jaffee**, Novartis (E); **T.P. Dryja**, Novartis (E); **S.-M. Liao**, Novartis (E)

References

1. Fritsche LG, Fariss RN, Stambolian D, Abecasis GR, Curcio CA, Swaroop A. Age-related macular degeneration: genetics and biology coming together. *Annu Rev Genomics Hum Genet*. 2014;15:151–171.

2. Black JR, Clark SJ. Age-related macular degeneration: genome-wide association studies to translation. *Genet Med*. 2016;16: 283–289.

3. Fritsche LG, Igl W, Bailey JN, et al. A large genome-wide association study of age-related macular degeneration highlights contributions of rare and common variants. *Nat Genet*. 2016;48:134–143.

4. Chen M, Xu H. Parainflammation, chronic inflammation, and age-related macular degeneration. *J Leukoc Biol*. 2015;98: 713–725.

5. Ambati J, Atkinson JP, Gelfand BD. Immunology of age-related macular degeneration. *Nat Rev Immunol*. 2013;13:438–451.

6. Tuo J, Grob S, Zhang K, Chan CC. Genetics of immunological and inflammatory components in age-related macular degeneration. *Ocul Immunol Inflamm*. 2012;20:27–36.

7. Knickelbein JE, Chan CC, Sen HN, Ferris FL, Nussenblatt RB. Inflammatory mechanisms of age-related macular degeneration. *Int Ophthalmol Clin*. 2015;55:63–78.

8. Klein RJ, Zeiss C, Chew EY, et al. Complement factor H polymorphism in age-related macular degeneration. *Science*. 2005;308:385–389.

9. Edwards AO, Ritter R III, Abel KJ, Manning A, Panhuysen C, Farrer LA. Complement factor H polymorphism and age-related macular degeneration. *Science*. 2005;308:421–424.

10. Haines JL, Hauser MA, Schmidt S, et al. Complement factor H variant increases the risk of age-related macular degeneration. *Science*. 2005;308:419–421.

11. Hageman GS, Anderson DH, Johnson LV, et al. A common haplotype in the complement regulatory gene factor H (HF1/CFH) predisposes individuals to age-related macular degeneration. *Proc Natl Acad Sci U S A*. 2005;102:7227–7232.

12. Zareparsi S, Branham KE, Li M, et al. Strong association of the Y402H variant in complement factor H at 1q32 with susceptibility to age-related macular degeneration. *Am J Hum Genet*. 2005;77:149–153.

13. Fagerness JA, Maller JB, Neale BM, Reynolds RC, Daly MJ, Seddon JM. Variation near complement factor I is associated with risk of advanced AMD. *Eur J Hum Genet*. 2009;17:100–104.

14. Gold B, Merriam JE, Zernant J, et al. Variation in factor B (BF) and complement component 2 (C2) genes is associated with age-related macular degeneration. *Nat Genet*. 2006;38:458–462.

15. Spencer KL, Hauser MA, Olson LM, et al. Protective effect of complement factor B and complement component 2 variants in age-related macular degeneration. *Hum Mol Genet*. 2007; 16:1986–1992.

16. Maller JB, Fagerness JA, Reynolds RC, Neale BM, Daly MJ, Seddon JM. Variation in complement factor 3 is associated with risk of age-related macular degeneration. *Nat Genet*. 2007;39:1200–1201.

17. Seddon JM, Yu Y, Miller EC, et al. Rare variants in CFI, C3 and C9 are associated with high risk of advanced age-related macular degeneration. *Nat Genet*. 2013;45:1366–1370.

18. Nishiguchi KM, Yasuma TR, Tomida D, et al. C9-R95X polymorphism in patients with neovascular age-related macular degeneration. *Invest Ophthalmol Vis Sci*. 2012;53:508–512.

19. Hughes AE, Orr N, Esfandiary H, Diaz-Torres M, Goodship T, Chakravarthy U. A common CFH haplotype, with deletion of CFHR1 and CFHR3, is associated with lower risk of age-related macular degeneration. *Nat Genet*. 2006;38:1173–1177.

20. Hageman GS, Hancox LS, Taiber AJ, et al. Extended haplotypes in the complement factor H (CFH) and CFH-related (CFHR) family of genes protect against age-related macular degeneration: characterization, ethnic distribution and evolutionary implications. *Ann Med*. 2006;38:592–604.

21. McHarg S, Clark SJ, Day AJ, Bishop PN. Age-related macular degeneration and the role of the complement system. *Mol Immunol*. 2015;67:43–50.

22. Anderson DH, Radeke MJ, Gallo NB, et al. The pivotal role of the complement system in aging and age-related macular degeneration: hypothesis re-visited. *Prog Retin Eye Res*. 2010;29:95–112.

23. Baudouin C, Peyman GA, Fredj-Reygrobellet D, et al. Immunohistological study of subretinal membranes in age-related macular degeneration. *Jpn J Ophthalmol*. 1992;36:443–451.

24. Scholl HP, Charbel Issa P, Walier M, et al. Systemic complement activation in age-related macular degeneration. *PLoS One*. 2008;3:e2593.

25. Smailhodzic D, Klaver CC, Klevering BJ, et al. Risk alleles in CFH and ARMS2 are independently associated with systemic complement activation in age-related macular degeneration. *Ophthalmology*. 2012;119:339–346.

26. Hecker LA, Edwards AO, Ryu E, et al. Genetic control of the alternative pathway of complement in humans and age-related macular degeneration. *Hum Mol Genet*. 2010;19:209–215.

27. Sivaprasad S, Adewoyin T, Bailey TA, et al. Estimation of systemic complement C3 activity in age-related macular degeneration. *Arch Ophthalmol*. 2007;125:515–519.

28. Reynolds R, Hartnett ME, Atkinson JP, Giclas PC, Rosner B, Seddon JM. Plasma complement components and activation fragments: associations with age-related macular degeneration genotypes and phenotypes. *Invest Ophthalmol Vis Sci*. 2009;50:5818–5827.

29. Stanton CM, Yates JR, den Hollander AI, et al. Complement factor D in age-related macular degeneration. *Invest Ophthalmol Vis Sci*. 2011;52:8828–8834.

30. Paun CC, Lechanteur YT, Groenewoud JM, et al. A novel complotype combination associates with age-related macular degeneration and high complement activation levels in vivo. *Sci Rep*. 2016;6:26568.

31. Schick T, Steinhauer M, Aslanidis A, et al. Local complement activation in aqueous humor in patients with age-related macular degeneration. *Eye*. 2017;31:810–813.

32. Tan X, Fujiu K, Manabe I, et al. Choroidal neovascularization is inhibited via an intraocular decrease of inflammatory cells in mice lacking complement component C3. *Sci Rep*. 2015;5:15702.

33. Poor SH, Qiu Y, Fassbender ES, et al. Reliability of the mouse model of choroidal neovascularization induced by laser photocoagulation. *Invest Ophthalmol Vis Sci*. 2014;55:6525–6534.

34. Rohrer B, Coughlin B, Kunchithapautham K, et al. The alternative pathway is required, but not alone sufficient, for retinal pathology in mouse laser-induced choroidal neovascularization. *Mol Immunol*. 2011;48:e1–e8.

35. Bora PS, Sohn JH, Cruz JM, et al. Role of complement and complement membrane attack complex in laser-induced choroidal neovascularization. *J Immunol*. 2005;174:491–497.

36. Pujol-Lereis LM, Schafer N, Kuhn LB, Rohrer B, Pauly D. Interrelation between oxidative stress and complement activation in models of age-related macular degeneration. *Adv Exp Med Biol*. 2016;854:87–93.

37. Rohrer B, Guo Y, Kunchithapautham K, Gilkeson GS. Eliminating complement factor D reduces photoreceptor susceptibility to light-induced damage. *Invest Ophthalmol Vis Sci*. 2007;48:5282–5289.

38. Woodell A, Coughlin B, Kunchithapautham K, et al. Alternative complement pathway deficiency ameliorates chronic smoke-induced functional and morphological ocular injury. *PLoS One*. 2013;8:e67894.

39. Troutbeck R, Al-Qureshi S, Guymer RH. Therapeutic targeting of the complement system in age-related macular degeneration: a review. *Clin Exp Ophthalmol*. 2012;40:18–26.

40. Volz C, Pauly D. Antibody therapies and their challenges in the treatment of age-related macular degeneration. *Eur J Pharm Biopharm*. 2015;95:158–172.

41. Hanus J, Zhao F, Wang S. Current therapeutic developments in atrophic age-related macular degeneration. *Br J Ophthalmol*. 2016;100:122–127.

42. Xu H, Chen M. Targeting the complement system for the management of retinal inflammatory and degenerative diseases. *Eur J Pharmacol*. 2016;787:94–104.

43. Mattapallil MJ, Wawrousek EF, Chan CC, et al. The Rd8 mutation of the Crb1 gene is present in vendor lines of C57BL/6N mice and embryonic stem cells, and confounds ocular induced mutant phenotypes. *Invest Ophthalmol Vis Sci*. 2012;53:2921–2927.

44. Wessels MR, Butko P, Ma M, Warren HB, Lage AL, Carroll MC. Studies of group B streptococcal infection in mice deficient in complement component C3 or C4 demonstrate an essential role for complement in both innate and acquired immunity. *Proc Natl Acad Sci U S A*. 1995;92:11490–11494.

45. Mueller-Ortiz SL, Drouin SM, Wetsel RA. The alternative activation pathway and complement component C3 are critical for a protective immune response against Pseudomonas aeruginosa in a murine model of pneumonia. *Infect Immun*. 2004;72:2899–2906.

46. Sivak JM, Ostriker AC, Woolfenden A, et al. Pharmacologic uncoupling of angiogenesis and inflammation during initiation of pathological corneal neovascularization. *J Biol Chem*. 2011;286:44965–44975.

47. Yang Z, Stratton C, Francis PJ, et al. Toll-like receptor 3 and geographic atrophy in age-related macular degeneration. *N Engl J Med*. 2008;359:1456–1463.

48. Koizumi K, Poulaki V, Doehmen S, et al. Contribution of TNF-alpha to leukocyte adhesion, vascular leakage, and apoptotic cell death in endotoxin-induced uveitis in vivo. *Invest Ophthalmol Vis Sci*. 2003;44:2184–2191.

49. Avunduk MC, Avunduk AM, Oztekin E, Baltaci AK, Ozyazgan Y, Mogolkoc R. Etanercept treatment in the endotoxin-induced uveitis of rats. *Exp Eye Res*. 2004;79:357–365.

50. Atkinson JP, Farries T. Separation of self from non-self in the complement system. *Immunol Today*. 1987;8:212–215.

51. Thurman JM, Holers VM. The central role of the alternative complement pathway in human disease. *J Immunol*. 2006;176:1305–1310.

52. Lachmann PJ. The amplification loop of the complement pathways. *Adv Immunol*. 2009;104:115–149.

53. Weisdorf DJ, Hammerschmidt DE, Jacob HS, Craddock PR. Rapid in vivo clearance of C5ades arg: a possible protective mechanism against complement-mediated tissue injury. *J Lab Clin Med*. 1981;98:823–830.

54. Lesavre PH, Muller-Eberhard HJ. Mechanism of action of factor D of the alternative complement pathway. *J Exp Med*. 1978;148:1498–1509.

55. Williams SC, Hinshelwood J, Perkins SJ, Sim RB. Production and functional activity of a recombinant von Willebrand factor-A domain from human complement factor B. *Biochem J*. 1999;342(pt 3):625–632.

56. Gorsuch WB, Chrysanthou E, Schwaeble WJ, Stahl GL. The complement system in ischemia-reperfusion injuries. *Immunobiology*. 2012;217:1026–1033.

57. Aredo B, Zhang K, Chen X, Wang CX, Li T, Ufret-Vincenty RL. Differences in the distribution, phenotype and gene expression of subretinal microglia/macrophages in C57BL/6N (Crb1 rd8/rd8) versus C57BL6/J (Crb1 wt/wt) mice. *J Neuroinflammation*. 2015;12:6.

58. Volanakis JE, Barnum SR, Giddens M, Galla JH. Renal filtration and catabolism of complement protein D. *N Engl J Med*. 1985;312:395–399.

59. Missel PJ. Simulating intravitreal injections in anatomically accurate models for rabbit, monkey, and human eyes. *Pharm Res*. 2012;29:3251–3272.

60. Botto M, Lissandrini D, Sorio C, Walport MJ. Biosynthesis and secretion of complement component (C3) by activated human polymorphonuclear leukocytes. *J Immunol*. 1992;149:1348–1355.

61. Reis ES, Barbuto JA, Isaac L. Human monocyte-derived dendritic cells are a source of several complement proteins. *Inflamm Res*. 2006;55:179–184.

62. Rutar M, Natoli R, Kozulin P, Valter K, Gatenby P, Provis JM. Analysis of complement expression in light-induced retinal degeneration: synthesis and deposition of C3 by microglia/macrophages is associated with focal photoreceptor degeneration. *Invest Ophthalmol Vis Sci*. 2011;52:5347–5358.

63. Ma W, Cojocaru R, Gotoh N, et al. Gene expression changes in aging retinal microglia: relationship to microglial support functions and regulation of activation. *Neurobiol Aging*. 2013;34:2310–2321.

64. Nitkiewicz J, Borjabad A, Morgello S, et al. HIV induces expression of complement component C3 in astrocytes by NF-kappaB-dependent activation of interleukin-6 synthesis. *J Neuroinflammation*. 2017;14:23.

65. Luo C, Chen M, Xu H. Complement gene expression and regulation in mouse retina and retinal pigment epithelium/choroid. *Mol Vis*. 2011;17:1588–1597.

66. Luo C, Zhao J, Madden A, Chen M, Xu H. Complement expression in retinal pigment epithelial cells is modulated by activated macrophages. *Exp Eye Res*. 2013;112:93–101.

67. Avichezer D, Grajewski RS, Chan CC, et al. An immunologically privileged retinal antigen elicits tolerance: major role for central selection mechanisms. *J Exp Med*. 2003;198:1665–1676.

68. Rose KL, Paixao-Cavalcante D, Fish J, et al. Factor I is required for the development of membranoproliferative glomerulonephritis in factor H-deficient mice. *J Clin Invest*. 2008;118:608–618.

69. Hong S, Beja-Glasser VF, Nfonoyim BM, et al. Complement and microglia mediate early synapse loss in Alzheimer mouse models. *Science*. 2016;352:712–716.

70. Johnson LV, Leitner WP, Staples MK, Anderson DH. Complement activation and inflammatory processes in drusen formation and age related macular degeneration. *Exp Eye Res*. 2001;73:887–896.

71. Zhou J, Kim SR, Westlund BS, Sparrow JR. Complement activation by bisretinoid constituents of RPE lipofuscin. *Invest Ophthalmol Vis Sci*. 2009;50:1392–1399.

72. Lad EM, Cousins SW, Van Arnam JS, Proia AD. Abundance of infiltrating CD163+ cells in the retina of postmortem eyes with dry and neovascular age-related macular degeneration. *Graefes Arch Clin Exp Ophthalmol*. 2015;253:1941–1945.

73. Gupta N, Brown KE, Milam AH. Activated microglia in human retinitis pigmentosa, late-onset retinal degeneration, and age-related macular degeneration. *Exp Eye Res*. 2003;76:463–471.

74. Cherepanoff S, McMenamin P, Gillies MC, Kettle E, Sarks SH. Bruch's membrane and choroidal macrophages in early and advanced age-related macular degeneration. *Br J Ophthalmol*. 2010;94:918–925.

75. Combadiere C, Feumi C, Raoul W, et al. CX3CR1-dependent subretinal microglia cell accumulation is associated with cardinal features of age-related macular degeneration. *J Clin Invest*. 2007;117:2920–2928.

76. Kleinman ME, Ambati J. Complement activation and inhibition in retinal diseases. *Dev Ophthalmol*. 2016;55:46–56.

77. Jack LS, Sadiq MA, Do DV, Nguyen QD. Emixustat and lampalizumab: potential therapeutic options for geographic atrophy. *Dev Ophthalmol*. 2016;55:302–309.

78. Le KN, Gibiansky L, Good J, et al. A mechanistic pharmacokinetic/pharmacodynamic model of factor D inhibition in cynomolgus monkeys by lampalizumab for the treatment of geographic atrophy. *J Pharmacol Exp Ther*. 2015;355:288–296.

79. Le KN, Gibiansky L, van Lookeren Campagne M, et al. Population pharmacokinetics and pharmacodynamics of lampalizumab administered intravitreally to patients with geographic atrophy. *CPT Pharmacometrics Syst Pharmacol*. 2015;4:595–604.

80. Rhoades W, Dickson D, Do DV. Potential role of lampalizumab for treatment of geographic atrophy. *Clin Ophthalmol*. 2015;9:1049–1056.

81. Roche. Roche Provides Update on First Lampalizumab Phase III Study for Geographic Atrophy, An Advanced Form of Age-Related Macular Degeneration (2017). Available at: https://www.roche.com/media/store/releases/med-cor-2017-09-08b.htm.

82. Loyet KM, Good J, Davancaze T, et al. Complement inhibition in cynomolgus monkeys by anti-factor d antigen-binding fragment for the treatment of an advanced form of dry age-related macular degeneration. *J Pharmacol Exp Ther*. 2014;351:527–537.

83. Nagai N, Oike Y, Noda K, et al. Suppression of ocular inflammation in endotoxin-induced uveitis by blocking the angiotensin II type 1 receptor. *Invest Ophthalmol Vis Sci*. 2005;46:2925–2931.

84. Gounarides J, Cobb JS, Zhou J, et al. Lack of involvement of CEP adducts in TLR activation and in angiogenesis. *PLoS One*. 2014;9:e111472.

85. Black PL, Hartmann D, Pennington R, et al. Effect of tumor burden and route of administration on the immunotherapeutic properties of polyinosinic-polycytidylic acid stabilized with poly-L-lysine in carboxymethyl cellulose [Poly(I,C)-LC]. *Int J Immunopharmacol*. 1992;14:1341–1353.

86. Sakurai M, Iigo M, Sasaki Y, et al. Lack of correlation between interferon levels induced by polyribonucleotides and their antimetastatic effect. *Oncology*. 1990;47:251–256.